gigacycle fatigue behaviors in Fusion Zone and Heat Affected Zone of Q345 LA steel welded joints

He Chao, Liu yongjie, Tian Renhui, Wang qingyuan
Dept of Civil Eng & Mechanics, Sichuan University, Chengdu 610065, Sichuan

Abstract: The fatigue behavior in Fusion Zone (FZ) and Heat Affected Zone (HAZ) of widely used low alloy steel, Q345, in very high cycle fatigue regime was experimentally studied with ultrasonic fatigue testing system. It was found that the fatigue failure of HAZ specimen still occurred beyond 10^7 cycles, while a horizontal platform was obtained for FZ specimen in VHCF regime related to internal welding defects in fusing zone. A high-sensitivity infrared imaging system was used to measure the temperature changes during fatigue testing and the relationship of temperature variation and fatigue damage was discussed. The temperature of BM specimen would rise rapidly with the beginning of crack propagation. Fatigue crack propagation lives of HAZ and FZ were estimated by monitoring the natural frequency of specimen, which was varying with the crack size during the fatigue testing. Results showed that more than 99% of the total fatigue life was occupied by the crack initiation process for base metal (BM) and HAZ. However, this number was scattered for FZ specimen at relatively low stress amplitude owing to the crack propagation from welding defects directly, without crack initiate life.

Keywords: VHCF, Welded Joints, Fatigue Crack Propagation Life, Heat Affected Zone, Fusion Zone

1. Introduction

In the applications of aircrafts, automobiles, off-shore structures and railway equipment, many components would experience nominal vibratory stress conditions over a long period of time, running up to several hundred million cycles in their working service [1,2]. Conventional fatigue design specifications address the stress at 10^7 cycles as the fatigue strength limit, which was not applicative for mechanical equipment working in super long life. By the statistics, the fatigue failure at welded joints accounted for over 80% of the total and became the most dangerous failure mode for welded structure [3]. The study on the fatigue behavior of welded joints is of significant importance.

The research on very high cycle fatigue has been an important issue with the development of ultrasonic fatigue test system. In recent years, many researchers have studied VHCF properties. Bathias et al.[4,5] made great contribution to the development of bending and torsion ultrasonic fatigue test system. Murakami et al. [6] proposed a semi-empirical model for high strength steel to predict the fatigue strength in considering of hardness, inclusion size and stress ratio. Wang et al. [7] analyzed the fatigue failure mechanism and predict the fatigue strength and fatigue life for six ultra-high strength steels. Xue et al. [8] and Huang et al. [9] studied the heat dissipation of specimen in VHCF with the help of infrared video camera. Marines et al. [10,11] proposed a model of fatigue crack propagation for internal “fish-eye” and surface crack initiation, based on the fatigue crack propagation law proposed by Paris [12].

In the past twenty years, most of the studies were performed on base materials, while fatigue behaviors of welded joints were rarely studied, especially in very high cycle fatigue domain. He et

al. [13] studied the gigacycle fatigue behavior of titanium alloy Ti-6Al-4V using ultrasonic fatigue at 20 kHz. Yin et al. [14] analyzed the fatigue failure mechanism of welded joint by SEM observation, and discussed the effect of ultrasonic peening treatment on the fatigue performance. In this paper, a special designed specimen was fatigued in very high cycle fatigue regime to investigate the fatigue performance of base metal, heat affected zone and fusion zone for steel Q345. A high-precision infrared video camera was used to measure the variation of surface temperature. The natural frequency changes of specimen were monitored to discuss the fatigue crack propagation lives of FZ and HAZ.

2. Material and experimental method

Table 1 Chemical composition of the base metal and solder (wt.%)

Material	C	Si	Mn	S	Alu	P	Mo	Fe
Q345q(Base metal)	0.15	0.38	1.36	0.00003	---	0.00012	0.00002	Rest
E45(Solder)	---	0861	2.236	---	0.648	---	1.569	Rest

Table 2 Mechanical properties of Q345 steel

E /GPa	σ_y/MPa	UTS/MPa	ρ/g.cm^{-3}	A/%	HV30
201	420	570	7.85	13	136

The material used in this study was a widely used low alloy steel, Q345, with yield strength of 420MPa. It's chemical composition and mechanical properties are presented in Table 1 and Table 2 respectively. With good tensile strength, plasticity, weld ability and low temperature deformability, Q345 steel has a widespread application in automobile, watercraft, pressure vessel etc.

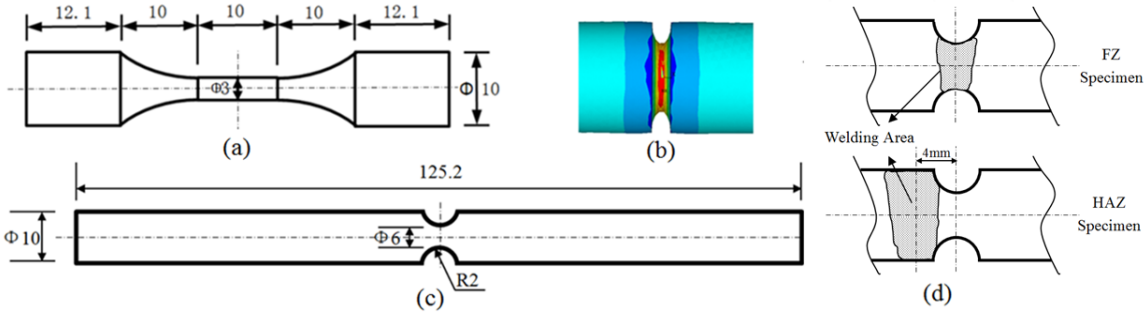

Fig.1 Specimens of ultrasonic fatigue test; (a) Parent specimen; (b) Stress field of welded joint specimen in mode analysis; (c) Dimensions of welded joint specimen; (d) schematic diagram of FZ and HAZ specimens

The dimensions of hourglass shape specimen for base metal are indicated in Fig2a.Welded joint specimen was machined from butt-welding plates with a thickness of 10mm. In ultrasonic fatigue test, the maximum stress always located in the middle of specimen. To ensure that the fracture section of HAZ and FZ specimen located in respective area, the center line of welding area

coincides with that of specimen length for FZ, while a distance of 4mm was designed between the center lines of welding area and HAZ specimen (Fig.1d). The radius of rounded roof for welded joint specimen was reduced to 2mm and other dimensions was determined by the method introduced in literature [15]. FEM results (shown in Fig.1b) showed that specially designed specimen was better to control the range of high stress area by restricting it at the root of arc during the test process. Fatigue test was performed on the USF-2000 ultrasonic fatigue test system (Fig.2) up to a limit of 10^9 load cycles under the conditions of stress ratio R=-1, at room temperature and compressed air cooling. The varying test resonance frequency of each specimen was measured by the computer control system. Moreover, an infrared thermometer was used to monitor the variations of temperature on the surface of specimen during test.

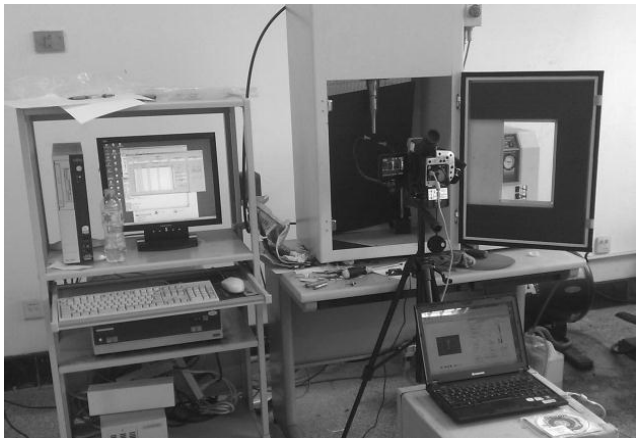

Fig.2 Ultrasonic fatigue test system with an infrared thermometer

3. Results and discussion

3.1 Summarizes of S-N curves

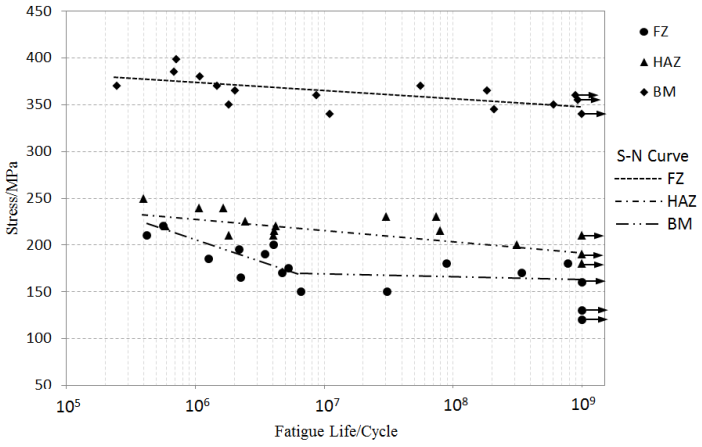

Fig.3 S-N fatigue curves of very high cycle fatigue test

Fig.3 presents the S-N curves for the three groups of specimens tested at room temperature in ultrasonic testing. Run out specimens over 10^9 cycles are represented by arrows. It was observed that that fatigue strength of HAZ and FZ was markedly lower than that of BM, with a percentage of 51.4% and 42.8% respectively at 10^9 cycles. Due to the local high temperature cycle in welding

process, unmatched mechanical properties and discontinuous microstructures between base metal and weld area were induced at the welded joint, which weakened the fatigue strength of welded structure significantly. It was confirmed from the observation of S-N curves of base metal and HAZ that failure continued to take place right up to gigacycle range (10^9 cycles) as mentioned in [3,8,16]. But for FZ specimen, a horizontal platform could be observed beyond 5.6×10^6 cycles. Because solder fill process caused welding defects such as micro cracks, pores and inclusions at fusing zone, fatigue crack propagated directly from thus defects without crack initiate life. If the loading stress is over the threshold of propagation, existing crack extent until final fracture rapidly in low cycle fatigue range In other case, the specimen would not fatigue to failure because of the insufficient for a new crack initiation at lower stress level. So the fatigue strength limit of FZ specimen existed, because no failure occurred below the stress of 150MPa.

3.2 Fractography analysis

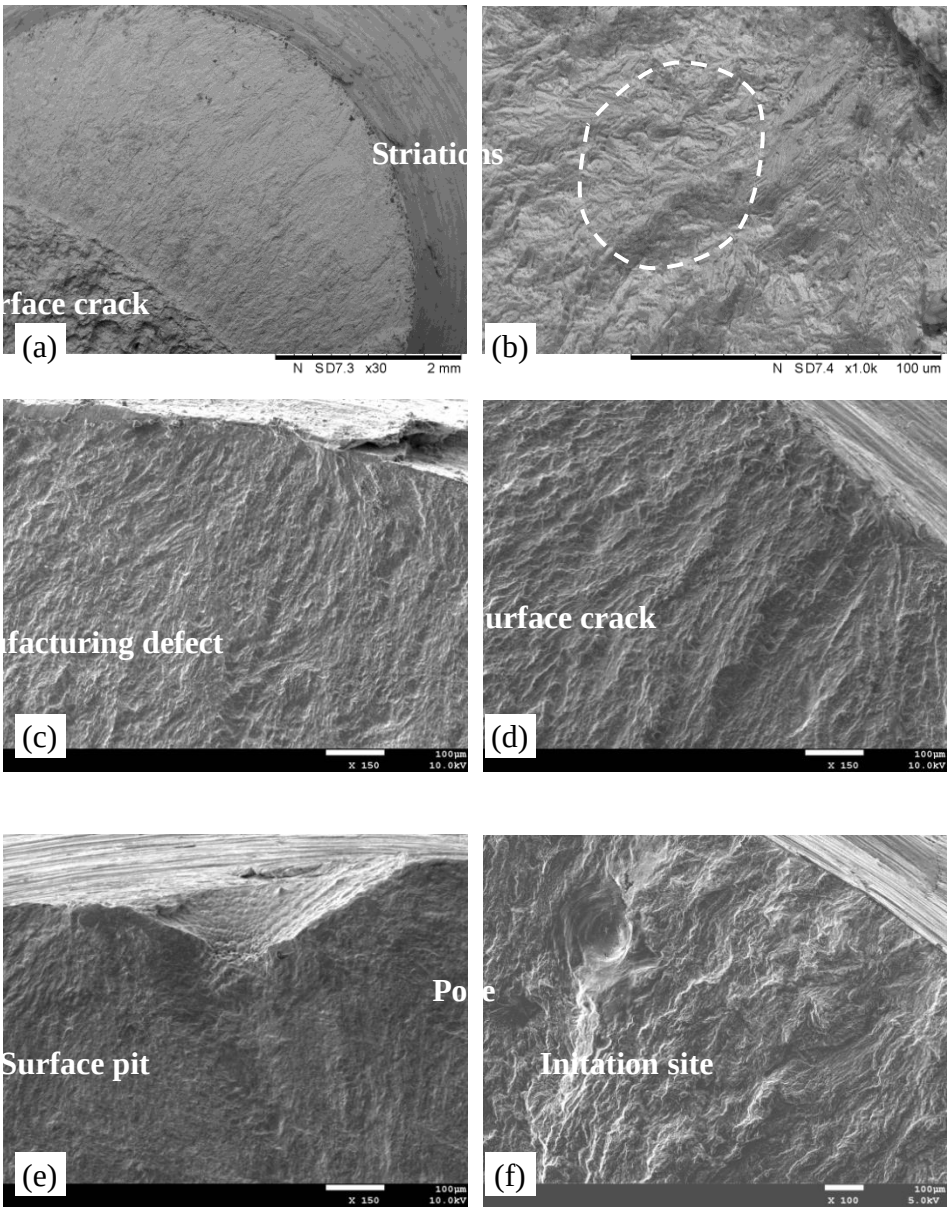

Fig.4 SEM fractographs of tested specimen; (a, b) Base metal specimen; (c, d) HAZ specimen; (e, f) FZ specimen

For high strength steel, it is known that the crack initiation and early propagation of interior-initiation fracture surface in VHCF range exhibit a pattern of “fish-eye” [17], a relatively rough region with fine granular morphology often presents surround the inclusion inside fish-eye. However, the fracture morphology of Q345 specimens in this test was different from high strength steel. Fig.5 illustrates the fatigue crack initiation modes based on SEM characterization. Due to the better plastic properties, the elongation of Q345 was much better than high strength steel. In addition, the stress at the surface was higher than internal, owing to the stress concentration effect caused by arc in the middle of the specimen. Local plastic deformation occurred more easily at the surface and fatigue cracks prone to start from surface of specimen for Q345 BM, which can be certified by the fatigue striations observed in Fig.4a and Fig.4b, around crack initiation site at the surface. The fatigue crack initiations of HAZ specimens were located at the surface (Fig.4c and d), which can be correlated to the local stress concentration at the retained surface defects caused by machining. For FZ specimens, cracks initiated from the welded defects such as pores and inclusions, as shown in Fig4 (e) and (f). Many researchers have reached an agreement that fatigue crack initiation process of base metal occupied over 99% of total fatigue life in very high cycle fatigue, but the fatigue cracks of FZ specimen begin to expand directly from existing welding defect, which reduced the crack initiation life. Therefore the fatigue strength of FZ specimen was much lower than that of base metal specimen and the crack propagation life in VHCF range will be discussed in the following sections.

3.3 The varying surface temperature of BM specimen

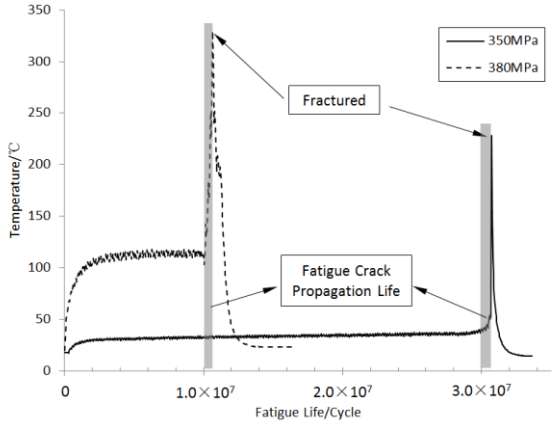

Fig.5 Temperature profiles of base metal specimen during testing.

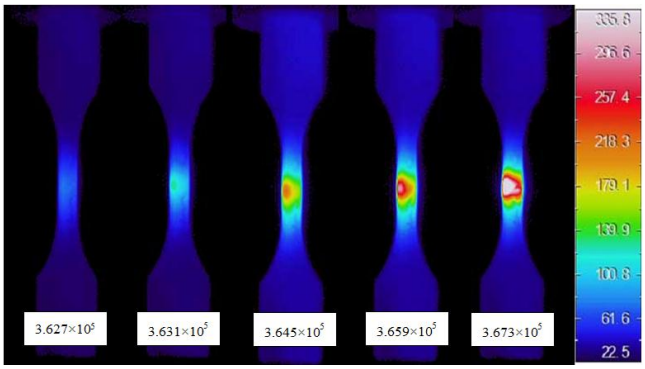

Fig.6 The rapidly increasing process of surface temperature for BM specimen

The surface temperature of specimen under high frequency is very complex including the effects of elastic strain energy, plastic strain energy, inelastic internal friction and heat dissipation [8,9,18]. An advanced infrared thermometer was used to monitor the variations of temperature on the surface of specimen during test. The temperature changes of weld specimen were not evident due to the low stress level and the larger waist diameter. But for BM specimens, it was found that the cyclic loading at an ultrasonic frequency generated a substantial amount of heat, and the temperature of BM specimen increased significantly at the center of the gage length of specimen as shown in Fig.6. The temperature distributions in the gage-length section of the specimen during ultrasonic testing were heterogeneous along the axis of the specimen, with the highest temperature occurring at the high strain location. Fig.5 illustrates the temperature variation at the center of the base metal specimen for two different stress levels without air cooling. The temperature increased evidently at the beginning of the test, which followed by a stable state. Thus stabilization could be explained by a balance between the mechanical energy dissipated into heat and the energy lost. The temperature was higher for higher stress loading. Fig.6 also shows that the temperature at the center of the specimen increased very sharply (3.627×10^6~3.673×10^6cycles) just before the fatigue failure occurred. Observation for fracture surface confirmed that the fatigue crack initiation site was located just on the point A plotted in Fig.6, which declared a close relation between the rise of temperature and crack propagation. XUE et al. [9] discussed that the dissipated energy came from internal material damping and the local plastic deformation at the microscopic scale, although the stress in the specimen is lower than the elastic limit. When the micro crack originated and started to propagate under cyclic loading, the plastic zone at the crack tip generated heat until the specimen fractured. Thus, the fatigue crack propagation life could be estimated by detecting the temperature variation of specimen and this will be discussed later.

3.4 The varying resonance frequency of welded joint specimen

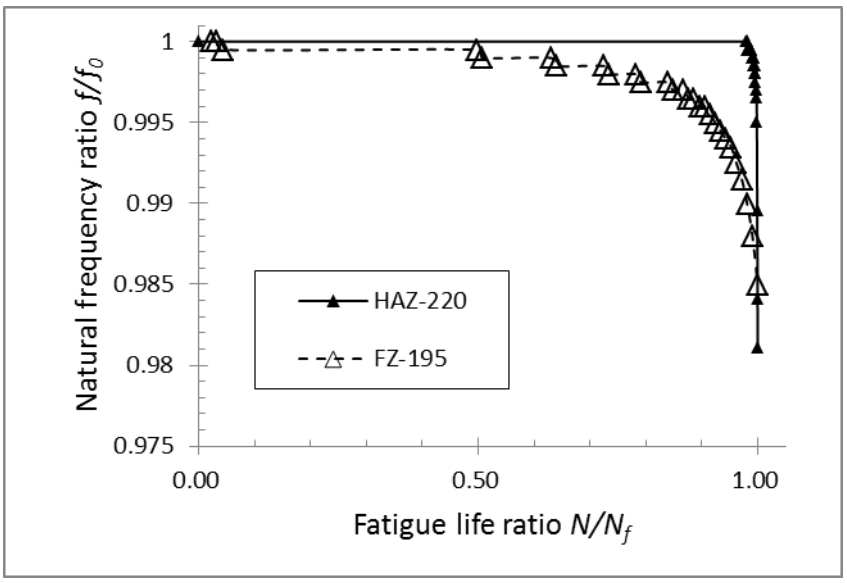

Fig.7 Natural frequency profiles of tested at different stress level.

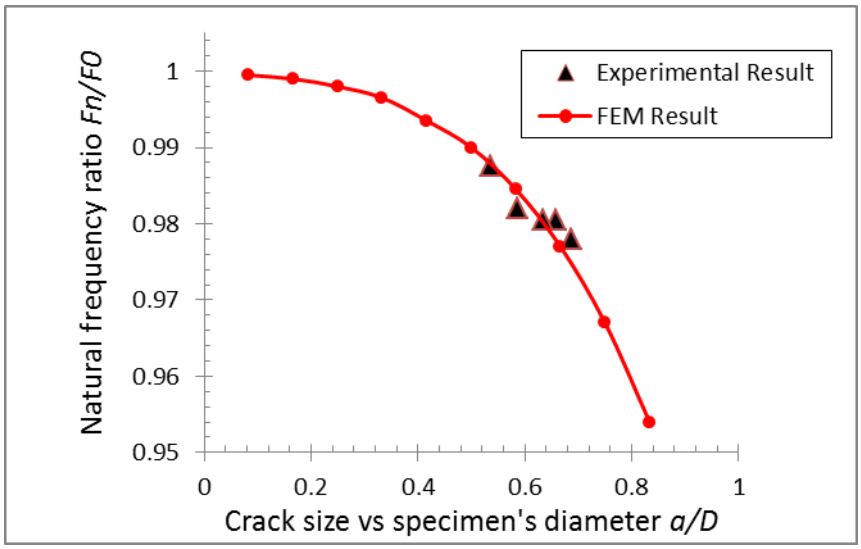

Fig.8 Comparison between the Finite element analysis values and the experimental results

It is interesting that a metallic noise could be heard just before the final fracture due to the decreasing of resonance frequency of welded joint specimen. The natural frequency of specimen was recorded per 20000 cycles in the course of the fatigue experiment and the changes of frequency in term of natural frequency ratio verse fatigue life ratio were shown in Fig.7, where N_f, f_0 were the final fatigue life and initial natural frequency, respectively. From the collected data of HAZ, a stable platform of natural frequency ratio could be observed, which occupied almost the whole fatigue life. Further, the fatigue life ratio was larger and the final stop frequency ratio for fracture was smaller with the higher loading stress. But for FZ specimen, the frequency ratio kept going down from the beginning of the test with no platform due to the fact that the frequency descent life was affected by the max size defect located in fusion zone. As mentioned previously, welded joint specimen fractured without obvious temperature-rise period, therefore, it could be due to the reason that fatigue propagation lead to the decreasing of natural frequency of welded joint. In order to verify, FEM model analysis method was employed to ascertain the relationship between natural frequency and fatigue crack size at the surface of specimen under the resonance condition. A half specimen model was established for computation time saving with a crack located in the middle section of the specimen. In the process of the resonance, the state of compression would result in crack surface contact, but any non-linear setting was not included in the analysis in ANSYS, which was neglected automatically, otherwise. To prevent the effect of crack surface compression on the analysis, an additional element layer with the thickness of 0.1mm was attached to the surface of fatigue crack. The modulus of elasticity for extra element is 1GPa, which was considerably less as compared to Q345.With the help of additional layer, the model of specimen remained linear without any penetrations of elements at the crack surface. After the model analysis of specimen with cracks in different sizes, the relation between fatigue crack size and natural frequency of welded joint specimen was obtained as presented in Fig.8. It could be found that with the increase in size of fatigue crack, the rate of natural frequency decreased. In this experiment, the final stop frequencies and max fatigue crack sizes from SEM observation were obtained on five HAZ specimens as plotted with solid triangle in Fig.9. It is noted that the experimental data just located near to the fitted curve of FEM, which confirmed that the decreasing of natural frequency was caused by the

fatigue crack propagation and fatigue crack propagation lives of HAZ and FZ could be estimated by monitoring the natural frequency of specimen.

3.5 The crack propagation lives of BM, HAZ and FZ specimens

Table 3 Fatigue crack propagation life of different specimens

Specimen	Stress/Mpa	Total life/cycle	Propagation Life/cycle	Ratio N_p/N_t
BM	350	6.08×10^8	1.72×10^6	0.28%
BM	365	1.83×10^8	7.27×10^5	0.40%
BM	370	5.60×10^7	1.66×10^5	0.29%
HAZ	200	3.12×10^8	8.8×10^5	0.28%
HAZ	220	7.42×10^7	5.8×10^5	0.78%
HAZ	230	3.02×10^7	3.0×10^5	0.99%
FZ	150	6.62×10^6	6.6×10^5	9.97%
FZ	185	1.26×10^6	9.6×10^5	76.2%
FZ	195	2.18×10^6	1.08×10^6	49.5%

The natural frequency of welded joint specimen was analysed in this section to clarify the fatigue crack propagation characteristic in VHCF range. It was believed that the fatigue crack start to grow at the moment that frequency of specimen decreased over 20Hz per 20000 cycles. For BM specimen, the period of temperature rise just before the fracture could be regarded as the crack propagation life, as discussed earlier. When the amplitude of temperature variation was larger than 5℃ per 700cycles, fatigue crack propagation was started for BM specimen. Finally, the fatigue crack propagation lives of BM, HAZ and FZ specimens were obtained in Table.3. Similar changes between BM and HAZ specimens were observed. It showed that with the increase in the loading stress, lower crack propagation life and ratio of propagation life to total fatigue life was obtained. The crack initiation process occupied over 99% of the total fatigue life for BM and HAZ in VHCF range. Therefore study on the mechanism of crack initiation was extremely important to clarify the fatigue properties in VHCF. In addition, the life ratio of FZ specimens were much larger than that of BM and HAZ, due to the fact that fatigue crack in FZ propagated directly from the welding defect with no apparent initiation process.

4. Conclusions

In this paper, ultrasonic fatigue test was performed on Q345 BM and welded joint to investigate the properties and failure mechanism in super long life fatigue range, the conclusions can be summarized as follows:

1.The fatigue strength of BM and HAZ continues to decline with the increase in fatigue live, and fatigue failure still occurred up to 10^9 cycles. Compared with BM specimen, the fatigue strength of FZ and HAZ decreased about 60% and 55% respectively.

2. The fatigue crack propagation process would lead to the temperature increment of BM and the decreasing of natural frequency descent in the test. Thus fatigue propagation life could be evaluated

by monitoring the changes of surface temperature and resonance frequency.

3. The crack initiation process occupied over 99% of the total fatigue life for BM and HAZ, but much larger for FZ specimens at relatively low stress amplitude. This was due to the reason that fatigue crack propagated directly from the welding defects for FZ specimen without apparent initiation process.

Acknowledgement

This work was financially supported by Chinese National Science Foundation (No.10925211). Thanks Prof. C. X. Huang for his guidance.

References

[1] Q.Y. Wang, C. Bathias, N. Kawagoishi, Q. Chen, Effect of inclusion on subsurface crack initiation and gigacycle fatigue strength, International Journal of Fatigue, Volume 24, Issue 12, December 2002, Pages 1269-1274

[2] Y Furuya, S Matsuoka, T Abe, K Yamaguchi, Gigacycle fatigue properties for high-strength low-alloy steel at 100 Hz, 600 Hz, and 20 kHz, Scripta Materialia, Volume 46, Issue 2, 18 January 2002, Pages 157-162, ISSN 1359-6462

[3] Lixing Huo, Dongpo Wang, Yufeng Zhang, Investigation of the fatigue behaviour of the welded joints treated by TIG dressing and ultrasonic peening under variable-amplitude load, International Journal of Fatigue, Volume 27, Issue 1, January 2005, Pages 95-101

[4] Claude Bathias, Piezoelectric fatigue testing machines and devices, International Journal of Fatigue, Volume 28, Issue 11, November 2006, Pages 1438-1445

[5] Z.D. Sun, C. Bathias, G. Baudry, Fretting fatigue of 42CrMo4 steel at ultrasonic frequency, International Journal of Fatigue, Volume 23, Issue 5, May 2001, Pages 449-453

[6] Yukitaka Murakami, Masayuki Takada, Toshiyuki Toriyama, Super-long life tension–compression fatigue properties of quenched and tempered 0.46% carbon steel, International Journal of Fatigue, Volume 20, Issue 9, October 1998, Pages 661-667

[7] Q.Y. Wang, M.R. Sriraman, N. Kawagoishi, Q. Chen, Fatigue crack growth of bonded composite repairs in gigacycle regime, International Journal of Fatigue, Volume 28, Issue 10, October 2006, Pages 1197-1201

[8] Zhi Yong Huang, Danièle Wagner, Qing Yuan Wang, Claude Bathias, Effect of carburizing treatment on the “fish eye” crack growth for a low alloyed chromium steel in very high cycle fatigue, Materials Science and Engineering: A, Volume 559, 1 January 2013, Pages 790-797

[9] H.Q. Xue, E. Bayraktar, C. Bathias, Damage mechanism of a nodular cast iron under the very high cycle fatigue regime, Journal of Materials Processing Technology, Volume 202, Issues 1–3, 20 June 2008, Pages 216-223

[10] Israel Marines-Garcia, Paul C. Paris, Hiroshi Tada, Claude Bathias, Fatigue crack growth from small to long cracks in very-high-cycle fatigue with surface and internal “fish-eye” failures for ferrite-perlitic low carbon steel SAE 8620, Materials Science and Engineering: A, Volumes 468–470, 15 November 2007, Pages 120-128

[11] Israel Marines-Garcia, Paul C. Paris, Hiroshi Tada, Claude Bathias, Fatigue crack growth from small to long cracks in VHCF with surface initiations, International Journal of Fatigue, Volume

29, Issues 9–11, September–November 2007, Pages 2072-2078

P.C. Paris, H. Tada, J.K. Donald.Service load fatigue damage – a historical perspective.Int. J. Fatigue, 21 (1999), pp. 35–46

[13] HE Chao, TIAN Ren-hui, WANG Qing-yuan, Study on ultra-long-life fatigue properties of welded joints under high-frequency loading, China Measurement & Test,Volume 38, Issues 3, May2012, Pages 20-26

[14] Danqing Yin, Dongpo Wang, Hongyang Jing, Lixing Huo, The effects of ultrasonic peening treatment on the ultra-long life fatigue behavior of welded joints, Materials & Design, Volume 31, Issue 7, August 2010, Pages 3299-3307

[15] Xue Hongqian. The design of specimen forfatigue test at ultrasonic frequency [J]. acta aeronautica ET Sstronautica Sinica, Volume 25, Issue 4, August 2004, Pages 425-428

[16] K. Shiozawa, Y. Morii, S. Nishino, L. Lu, Subsurface crack initiation and propagation mechanism in high-strength steel in a very high cycle fatigue regime, International Journal of Fatigue, Volume 28, Issue 11, November 2006, Pages 1521-1532

[17] Claude Bathias, Paul C. Paris, Gigacycle fatigue of metallic aircraft components, International Journal of Fatigue, Volume 32, Issue 6, June 2010, Pages 894-897, ISSN 0142-1123

[18] N. Ranc, D. Wagner, P.C. Paris, Study of thermal effects associated with crack propagation during very high cycle fatigue tests, Acta Materialia, Volume 56, Issue 15, September 2008, Pages 4012-4021